ISSN 1027-5495. Functional Materials, 26, No.4 (2019), p. 703-709.
doi:https://doi.org/10.15407/fm26.04.703

Synthesis of $ZnWO_4:Eu^{3+}$ and $Zn_xMg_{1-x}WO_4:Eu^{3+}$ X-ray-excitable phosphor nanoparticles

***I.A.Tupitsyna*[1,4], *A.G.Yakubovskaya*[1,4], *A.N.Puzan*[3], *O.M.Vovk*[2]**

[1]Institute for Scintillation Materials, STC "Institute for Single Crystals", National Academy of Sciences of Ukraine,
[2]Institute for Single Crystals, STC "Institute for Single Crystals", National Academy of Sciences of Ukraine,
[3]SSI "Institute for Single Crystals", STC "Institute for Single Crystals", National Academy of Sciences of Ukraine,
60 Nauky Ave., 61072 Kharkiv, Ukraine
[4]V.N.Karazin Kharkiv National University, 4 Svobody Sq., 61022 Kharkiv, Ukraine

Received September 15. 2019

$ZnWO_4:Eu^{3+}$ and $Zn_xMg_{1-x}WO_4:Eu^{3+}$ nanoparticles were obtained by the microwave-hydrothermal and the flux methods. The optimal conditions for obtaining nanocrystals with bright luminescence in the "red" spectral region are determined. The X-ray luminescence intensity of the 614 nm band for $ZnWO_4:Eu^{3+}$ and $Zn_{0.685}Mg_{0.285}Eu_{0.03}WO_4$ nanoparticles are 71 % and 108 %, respectively, versus the 500 nm intrinsic X-ray luminescence intensity of $ZnWO_4$ single crystal. $ZnWO_4:Eu^{3+}$ and $Zn_xMg_{0.97-x}Eu_{0.03}WO_4$ scintillation nanomaterials are promising for luminescent tomography for visualization of biological objects.

Keywords: tungstate nanocrystals, X-ray phosphor, luminescent tomography.

Получены нанокристаллы $ZnWO_4:Eu^{3+}$ и $Zn_xMg_{1-x}WO_4:Eu^{3+}$ гидротермальным микроволновым методом и раствор-расплавным методом. Определены оптимальные условия получения нанокристаллов с ярким свечением в красной области спектра. Нанокристаллы $ZnWO_4:Eu^{3+}$ и $Zn_{0.685}Mg_{0.285}Eu_{0.03}WO_4$ имеют интенсивность рентгенолюминесценции в полосе 614 нм 71 % и 108 %, соответственно, от интенсивности собственной рентгенолюминесценции при $\lambda = 500$ нм монокристаллического образца $ZnWO_4$. Сцинтилляционные наноматериалы $ZnWO_4:Eu^{3+}$ и $Zn_xMg_{1-x}WO_4:Eu^{3+}$ перспективны для использования в люминесцентной томографии для визуализации биологических объектов.

Синтез наночастинок рентгенолюмінофорів $ZnWO_4:Eu^{3+}$ і $Zn_xMg_{1-x}WO_4:Eu^{3+}$. *І.А.Тупіцина, Г.Г.Якубовська, А.М.Пузан, О.М.Вовк.*

Отримано нанокристали $ZnWO_4:Eu^{3+}$ і $Zn_xMg_{1-x}WO_4:Eu^{3+}$ гідротермальним мікрохвильовим методом і розчин-розплавним методом. Визначено оптимальні умови отримання нанокристалів з яскравим світінням в "червоній" області спектра. Нанокристали $ZnWO_4:Eu^{3+}$ і $Zn_{0.685}Mg_{0.285}Eu_{0.03}WO_4$ мають інтенсивність рентгенолюмінесценції у смузі 614 нм 71 % і 108 %, відповідно, від інтенсивності власної рентгенолюмінесценції при $\lambda = 500$ нм монокристалічного зразка $ZnWO_4$. Сцинтиляційні наноматеріали $ZnWO_4:Eu^{3+}$ і $Zn_xMg_{1-x}WO_4:Eu^{3+}$ перспективні для використання у люмінесцентній томографії для візуалізації біологічних об'єктів.

1. Introduction

X-ray fluorescence imaging is a new method of biomedical imaging [1–5]. However, nowadays the sensitivity of research equipment is insufficient, which leads to low spatial resolution. The combination of this method with the possibility of using nanoparticles as a contrast medium demonstrates the opportunity for improving of research equipment functional parameters [6]. It is known that nanoparticles selectively accumulate in the tumor (enhanced penetration and retention (EPR) effect) [7, 8], and it can lead to a significant increase in detectability research capacity. The luminescence excited with X-rays radiation allows to visualize the deep-lying tumors. In this method, the nanoparticles with red and near infrared X-ray excited emissions (~ 600–1400 nm) should be used in the so-called biological tissue transparency window [9]. In the mentioned spectral region, the absorption coefficients of water, melanin, desoxy- and hemoglobin (of blood) are low. The development of the methods using the X-ray luminescence tomography for visualizing biological objects was the driving force for the search of new X-ray-excitable phosphors [10–15], in particular the attention was paid to the Ln^{3+}-doped nanoparticles.

The scintillation materials based on $ZnWO_4$ attract particular attention because its X-ray luminescence parameters close to those of cadmium tungstate while it has not toxicity.

Several synthesis methods for obtaining $ZnWO_4$ nanoparticles were introduced earlier: sol-gel [16, 17], hydrothermal [18], solvotermal [19, 20], molten salt (flux) [21], microemulsion-based synthesis [22] etc. Hydrothermal synthesis with microwave heating makes it possible to quickly obtain products of a required morphology and dispersion with a narrow particle size distribution and a high degree of purity. We have previously shown that $ZnWO_4$ nanocrystals obtained by the flux method in lithium nitrate have the most intense X-ray luminescence [23]. In addition, we obtained by this method and investigated mixed $Zn_xMg_{1-x}WO_4$ nanocrystals [24]. The effect of light output increasing for the mixed $Zn_xMg_{1-x}WO_4$ single crystals, with a maximum at $x = 0.5$ [25], was also found for nanocrystals of the same composition [24]. However, an anomalous increasing of this effect more than three times was shown at transition to nanoscale sizes.

The aim of the work was to obtain $ZnWO_4:Eu^{3+}$ and $Zn_xMg_{1-x}WO_4:Eu^{3+}$ nanoparticles as X-ray-excitable phosphor in the "red" region.

2. Experimental

2.1 Synthesis of nanoparticles

Hydrothermal synthesis with microwave heating

We used the following starting materials: $Na_2WO_4 \cdot 2H_2O$ (special purity grade), $Zn(NO_3)_2 \cdot 6H_2O$ (reagent grade), $NH_3 \cdot H_2O$ of analytical grade purity (98 %), HNO_3 (99.99 %) manufactured by Merk, EuO (99.999 %) manufactured by Sigma-Aldrich. $Eu(NO_3)_3 \cdot 6H_2O$ was prepared by dissolving EuO with concentrated nitric acid. All solutions were prepared in distilled water without additional purification of the starting materials.

Initially, amorphous precipitate was prepared by co-precipitation of 0.1 M aqueous solutions of nitrates and Na_2WO_4 at the room temperature with vigorous stirring. pH of solutions was adjusted by adding dilute aqueous solutions of 30 % $NH_3 \cdot H_2O$. The synthesis was carried out by microwave hydrothermal method on microwave installation MARS (GEM Corporation Matthews, USA) at the temperature of 200°C and frequency of 2,45 GHz for 30 min. The synthesis temperature was previously determined in experiments on the preparation of undoped $ZnWO_4$ nanocrystals [26]. Upon completion of the synthesis the white precipitate was filtered, washed with distilled water and dried at 80°C in air for 3 h.

Flux synthesis

For the synthesis, we used zinc and europium nitrates, sodium tungstate, described above, and $Mg(NO_3)_2 \cdot 6H_2O$, which was prepared by dissolving MgO (special purity grade) in concentrated nitric acid.

$Zn_xMg_{1-x}WO_4:Eu^{3+}$ nanocrystals were obtained by crystallization of amorphous precipitate in molten salt of $LiNO_3$ [24]. Initially, amorphous $Zn_xMg_{1-x}WO_4:Eu^{3+}$ samples were obtained by co-precipitation of 0.1 M aqueous solutions of nitrates (and corresponding amount of europium nitrate) and Na_2WO_4 at the room temperature with vigorous stirring. The purified and dried precipitates were mixed with lithium nitrate in a weight ratio of 1:10 and melted at 300°C, followed by exposure for 16 h. The reaction product was washed, filtered and dried at 80°C in air.

2.2 Characterization

X-ray phase analysis of the samples was characterized by X-ray powder diffraction (XRD) on Siemens D-500 powder diffractometer (radiation Cu–Kα, λ = 1.54184 Å, secondary beam graphite monochromator, Bragg-Brentano geometry).

Morphology of the nanocrystals was investigated by transmission electron microscopy (TEM) using EM-125 (SELMA, Ukraine) microscope. Electron accelerating voltage was 125 kV, the survey was carried out in the bright field mode, and the image was recorded by CCD matrix.

The X-ray luminescence spectra of the nanocrystals were recorded by means of spectrometric complex KSVU-23. X-ray source REYS (U_a≤40 keV, I_a≤50 μA) was used as an excitation.

3. Result and discussion

3.1 $ZnWO_4$:Eu^{3+} nanoparticles, obtained by hydrothermal synthesis with microwave heating

The samples of $ZnWO_4$:Eu^{3+} nanoparticles were obtained ($C_{Eu^{3+}}$ = 0.5, 1, 7, 10 at.%) and the effect of the pH of the solution on the phase composition and morphology of zinc tungstate nanocrystals was studied.

XRD patterns proved that all nanocrystals are monophasic with a wolframite-type monoclinic structure of $ZnWO_4$ (JCDPS No. 15-0774). However, for samples with = 7 and 10, a noticeable shift in the position of the XRD lines is observed. This indicates a change in the crystal lattice parameters due to Eu3+ entering to the lattice (Fig. 1).

Earlier, we showed that microwave synthesis of undoped $ZnWO_4$ at 200°C lead to formation of nanoparticles in the shape of "grains" 25–50 nm (pH of solution is 5.5–6.2) and "rods" 250–300 nm in length and 30 nm in diameter (pH ~ 8–9.5) [26]. This morphology of nanoparticles is associated with a predominant growth by one of the crystallographic directions due to the anisotropic structure of $ZnWO_4$.

The TEM-analysis of $ZnWO_4$:Eu^{3+} nanoparticles showed that pH ~ 6.2 of solution leads to the formation of nanoparticles with a diameter of about 10 nm and a length of 30÷50 nm in case of $C_{Eu^{3+}}$ = 0.5 % and a diameter of about 20 nm and a length of 50 nm in case of $C_{Eu^{3+}}$ = 7 % (Fig. 2). Significant increasing of $ZnWO_4$:Eu^{3+} nanoparticles length, as well as for $ZnWO_4$ [26], are observed when pH of solution increase to 8. For a small concentration of Eu^{3+} (0.5 % and 1 %) at pH ~ 8 the nanoparticle sizes are ∅(15–20) nm×(150–180) nm. A slight increasing of particles to ∅25 nm ×(150–180) nm is observed with an increasing of europium concentration up to 7 %, however, at $C_{Eu^{3+}}$ = 10 % grains with a size of about 10 nm are formed. The doping of $ZnWO_4$ by europium slightly accelerates diffusion and leads to a small increasing of nanoparticles size (Fig. 2a and b, c and e). But this is observed only for $C_{Eu^{3+}}$ = 0.5÷7 %. With a further increasing of the europium concentration up to $C_{Eu^{3+}}$ = 10 %, a sharp slowdown of nanocrystals growth and a decreasing of grain size by more than 10 times are observed.

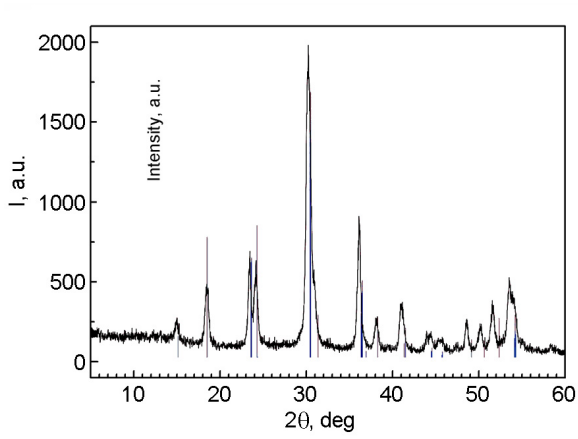

Fig. 1. X-ray diffraction patterns of $ZnWO_4$ (7 % Eu^{3+}) nanocrystals obtained at pH ~ 8 and 200 °C by microwave-hydrothermal synthesis. Vertical lines correspond to the position of the peaks of $ZnWO_4$ according to JCDPS No. 15-0774.

Measurement of the X-ray luminescence spectra of samples of $ZnWO_4$:Eu^{3+} nanocrystals with $C_{Eu^{3+}}$ = 1 % showed an increasing of the luminescence intensity by more than 3 times when pH increase from 6.2 to 8 (Fig. 3a). Such a trend is observed both in the 500 nm band due to the intrinsic luminescence band of the WO_6 complex and in the luminescence bands associated with transitions of $^5D_0 \rightarrow {}^7F_j$ to Eu^{3+} ions. The most intensive peak of 614 nm corresponds to the intracenter transition $^5D_0 \rightarrow {}^7F_2$.

The photoluminescence of $ZnWO_4$:Eu^{3+} has been studied quite well, since this material is promising as a white phosphor [27]. It was shown in these works that energy transfer from tungsten luminescence center to Eu^{3+}

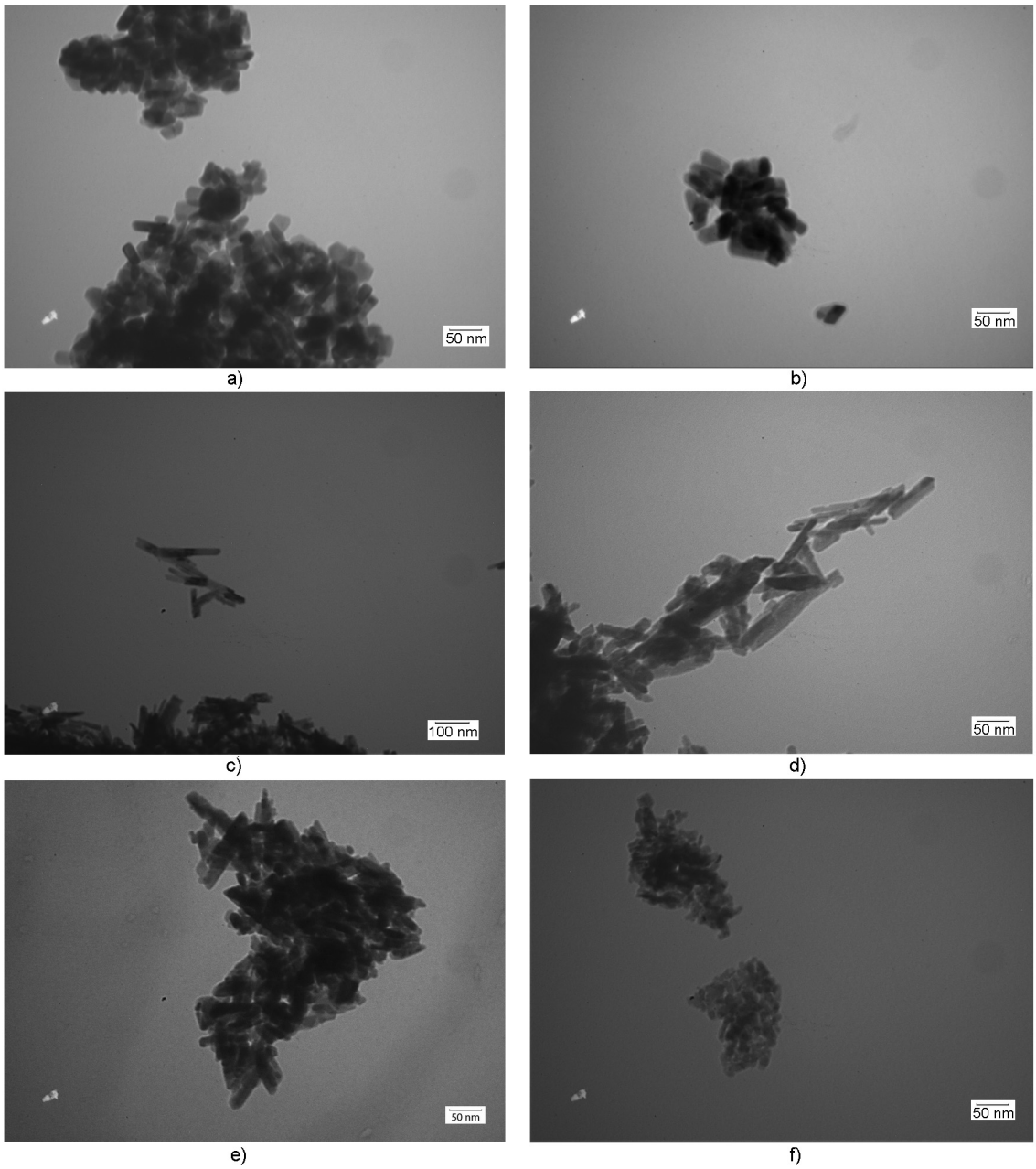

Fig. 2. TEM images of $ZnWO_4$:Eu^{3+} nanocrystals with different Eu^{3+} concentrations obtained from solutions with different pH: a) $ZnWO_4$(0.5 % Eu) pH 6.2, b) $ZnWO_4$ (7 % Eu) pH 6.2, c) $ZnWO_4$ (0.5 % Eu) pH 8, d) $ZnWO_4$ (1 % Eu) pH 8, e) $ZnWO_4$ (7 % Eu) pH 8, f) $ZnWO_4$ (10 % Eu) pH 8.

upon photoexcitation (λ_{ex} = 280 nm, 330 nm) is observed. It was found that in the photoluminescence spectra of $ZnWO_4$:Eu^{3+} with an increasing of europium concentration, the intensity of the 470 nm band decreases and the intensity of the Eu^{3+} band in the "red" region of the spectrum increases [27]. We do not observe such an exact correlation for the X-ray luminescence spectra of samples with different concentrations of europium (Fig. 3b) since, in addition to the process of energy transfer, we showed that for $ZnWO_4$ nanocrystals there is a direct relationship between the size of the nanoparticle and the X-ray luminescence intensity [28]. The test samples had differences in size (Fig. 2c–f).

For $ZnWO_4$:Eu^{3+} samples obtained from solutions with pH ~ 8, the increasing of europium concentration from 0.5 % up to 7 % leads to increasing of luminescence intensity, especially the 614 nm band. When the europium concentration increases up to

Table 1. The X-ray luminescence intensity at λ_{max} of the $ZnWO_4$ single crystal and $ZnWO_4:Eu^{3+}$ nanocrystals obtained from solutions with pH ~ 8

Sample	X-ray luminescence intensity at λ_{max} = 500 nm, a.u.	X-ray luminescence intensity at λ_{max} = 614 nm
$ZnWO_4$ crystal	1	0.1
$ZnWO_4$:Eu(0.5 %)	0.03	0.07
$ZnWO_4$:Eu(1 %)	0.02	0.10
$ZnWO_4$:Eu(7 %)	0.02	0.71
$ZnWO_4$:Eu(10 %)	0.01	0.39

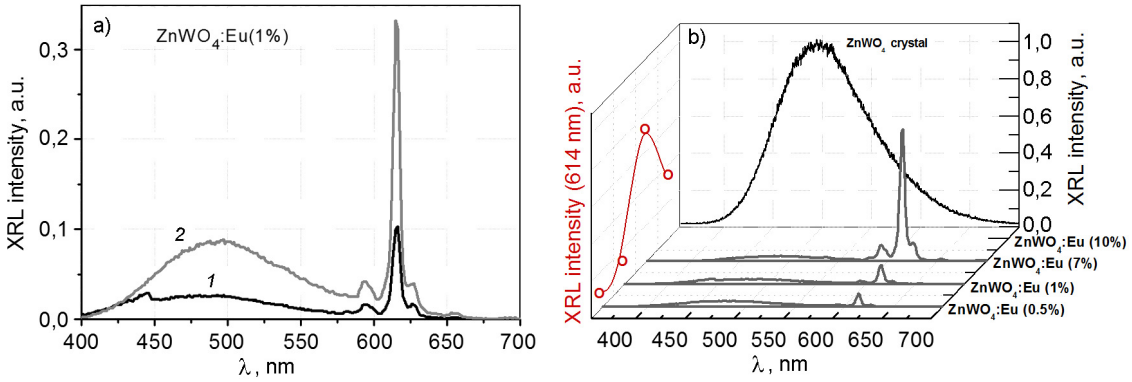

Fig. 3. X-ray luminescence spectra of $ZnWO_4:Eu^{3+}$ nanocrystals: a) C_{Eu}^{3+} = 1 %, (1) — obtained from solutions with pH ~ 6.2, (2) — pH ~ 8; b) obtained from solutions with pH ~ 8 and the spectrum of a $ZnWO_4$ single crystal.

10 %, a decreasing of the luminescence intensity of europium is observed, which may be due to both quenching and a decreasing of nanoparticles size, as was found for $ZnWO_4$ nanoparticles [28]. In favor of the latter assumption, it is intensity decreasing of the main luminescence band λ = 500 nm is observed for $ZnWO_4:Eu^{3+}$ nanocrystals with C_{Eu}^{3+} = 10 %. Table 1 shows the X-ray luminescence intensities of $ZnWO_4:Eu^{3+}$ nanocrystals obtained from solutions with pH ~ 8 versus data for $ZnWO_4$ single crystal. The intensity of "red" luminescence band for $ZnWO_4:Eu^{3+}$ nanocrystals with C_{Eu}^{3+} = 7 % is comparable with the intrinsic luminescence of the $ZnWO_4$ single crystal and is equal to 71 %.

3.2 Flux synthesis of tungstate nanocrystals

The mixed nanocrystals of zinc and magnesium tungstates doped with europium were obtained in this work by the flux method. XRD patterns proved that all $Zn_xMg_{0.97-x}Eu_{0.03}WO_4$ nanocrystals are monophasic with a wolframite-type monoclinic structure (JCDPS No. 15-0774). The TEM-analysis of nanoparticles showed that samples of different compositions are grains with a size of up to 200 nm. We did not observe correlations of the composition of nanoparticles and grain sizes. The TEM image of $Zn_{0.485}Mg_{0.485}Eu_{0.03}WO_4$ nanoparticles is shown in Fig. 4.

In [24], we showed that for undoped mixed nanocrystals of zinc and magnesium tungstate was found 4.5-fold increasing of the X-ray luminescence intensity for $Zn_{0.5}Mg_{0.5}WO_4$ versus $ZnWO_4$ [24]. This is due to the observed a non-linear dependence of the oxygen vacancy concentration on the ratio of zinc and magnesium cations in $Zn_xMg_{1-x}WO_4$ nanocrystals with a minimum for $Zn_{0.5}Mg_{0.5}WO_4$ sample. Oxygen vacancies in mixed crystals lead to lattice distortion and formation of a nonradiative relaxation channel competing with the WO_6^{6-} luminescence center that reduce the luminescence intensity of the main band.

The X-ray luminescence spectra of $Zn_xMg_{0.97-x}Eu_{0.03}WO_4$ nanoparticles are a superposition of the intrinsic luminescence band of wolframite with λ_{max} = 500 nm and the transition bands to Eu^{3+} (Fig. 5). There are also shows the spectrum of $ZnWO_4$ sin-

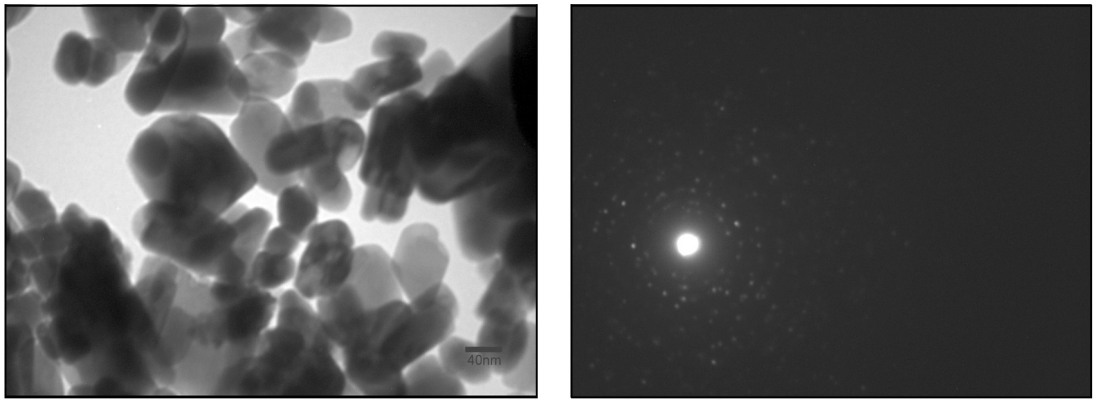

Fig. 4. TEM-image and diffraction pattern of $Zn_{0.485}Mg_{0.485}Eu_{0.03}WO_4$.

gle crystal. The X-ray luminescence intensities of all the $Zn_xMg_{0.97-x}Eu_{0.03}WO_4$ samples were calculated versus the parameter of $ZnWO_4$ single crystal (shown in Table 2). The dependence of the X-ray luminescence intensity at $\lambda_{max} = 614$ nm on the composition of mixed nanocrystal is nonlinear and has a maximum for the $Zn_{0.685}Mg_{0.285}Eu_{0.03}WO_4$ sample. The X-ray luminescence intensity of this sample at $\lambda = 614$ nm is slightly higher than the intrinsic X-ray luminescence intensity ($\lambda = 500$ nm) of $ZnWO_4$ single crystal, which makes this material promising for luminescent tomography of biological objects.

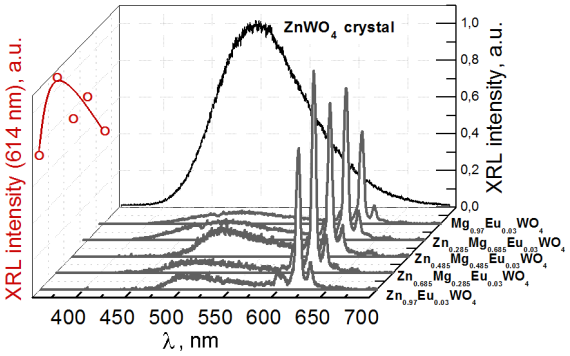

Fig. 5. X-ray luminescence spectra of $Zn_xMg_{0.97-x}Eu_{0.03}WO_4$ nanocrystals obtained by the flux method.

4. Conclusions

The nanosized $ZnWO_4:Eu^{3+}$ were obtained by the hydrothermal-microwave method with varying europium concentration and preparation conditions. XRD, TEM images, and X-ray luminescence of the samples were studied. The most intense X-ray luminescence in the "red" region of the spectrum was observed for the sample with 7 % of Eu^{3+}, which was prepared in the solution with pH ~ 8 at 200°C. The X-ray luminescence intensity of the 614 nm band for the sample is 71 % versus the 500 nm intrinsic X-ray luminescence band of $ZnWO_4$ single crystal.

$Zn_xMg_{0.97-x}Eu_{0.03}WO_4$ mixed nanocrystals were obtained by the flux method and their complex study was carried out. The intensity dependence of the "red" X-ray luminescence band (614 nm) on the composition of the mixed nanocrystal is nonlinear and has a maximum for the $Zn_{0.685}Mg_{0.285}Eu_{0.03}WO_4$ sample. The X-ray luminescence intensity of

Table 2. The X-ray luminescence intensity at λ_{max} of the $ZnWO_4$ single crystal and $Zn_xMg_{0.97-x}Eu_{0.03}WO_4$ nanocrystals (obtained by the flux method)

Sample	X-ray luminescence intensity at $\lambda_{max} = 500$ nm, a.u.	X-ray luminescence intensity at $\lambda_{max} = 614$ nm, a.u.
$ZnWO_4$ crystal	1	0.1
$Zn_{0.97}Eu_{0.03}WO_4$	0.07	0.76
$Zn_{0.685}Mg_{0.285}Eu_{0.03}WO_4$	0.06	1.08
$Zn_{0.485}Mg_{0.485}Eu_{0.03}WO_4$	0.12	0.79
$Zn_{0.285}Mg_{0.685}Eu_{0.03}WO_4F255$	0.10	0.80
$Mg_{0.97}Eu_{0.03}WO_4$	0.06	0.49

this sample at $\lambda = 614$ nm exceeds the intensity of intrinsic X-ray luminescence ($\lambda_{max} = 500$ nm) of $ZnWO_4$ single crystal.

The obtained scintillation nanomaterials are promising for luminescent tomography for visualization of biological objects.

References

1. G.Pratx, C.M.Carpenter, C.Sun et al., *Opt. Lett.*, **35**, 3345 (2010).
2. D.Chen, F.Meng, F.Zhao et al., *BioMed Res. Intern., 1 (2016).*
3. P.Gao, J.Rong, H.Pu et al., *Opt. Express*, **26**, 23233 (2018).
4. D.Chen, C.A.Dougherty, D.Yang et al., *Tomography*, **2**, 3 (2016).
5. D.Chen, S.Zhu, X.Chen et al., *Appl. Phys. Lett.*, **105**, 191104 (2014)
6. J.C.Larsson, C.Vogt, W.Vagberg et al., *Phys. Med. Biol.*, **63**, 164001 (2018)
7. R.Duncan, Y.-N.Sat, *Ann. Oncol.*, **9**, 39(1998).
8. H.Maeda, *J. Control Release*, **164**, 138 (2012).
9. S.Stolik, J.A.Delgado, A.Perez et al., *J. Photochem. Photobiol, B*, **57**, 90 (2000).
10. L.Sudheendra, G.K.Das, C.Li et al., *Chem. Mater.*, **26**, 1881 (2014).
11. S.Dufort, L.Sancey, C.Wenk et al., *BBA Biomembranes*, **1798**, 2266 (2010).
12. Y.Yang, Q.Shao, R.Deng et al., *Angew. Chem., Int, Ed.*, **51**, 3125 (2012).
13. L.Huo, J.Zhou, R.Wu et al., *Opt. Mater. Express*, **6**, 1056 (2016).
14. M.Alkahtani, Y.Chen, J.J. Pedraza et al., *Opt.Express*, **25**, 1030 (2017).
15. Z.Yi, W.Lu, C.Qian et al., *Biomater. Sci.*, **2**, 1404 (2014).
16. M.Rahmani, T.Sedaghat, *J. Inorg. Organomet. Polym.*, **29**, 220 (2019).
17. Y.Wu, S.C.Zhang, L.W.Zhang et al., *Chem. Res. Chin. Univ.*, **23**, 465 (2007).
18. S.J.Chen, J.H.Zhou, X.T.Chen et al., *Chem. Phys. Lett.*, **375**, 185 (2003).
19. C.Di, S.Guozhen, T.Kaibin et al., Elsevier, v.8, 1783 (2003).
20. J.Bi, L.Wu, Z.Ding et al., *J. Alloys Compd.*, **480**, 684 (2009).
21. J.Xiaohui, M.Junfeng, L.Jun et al., Elsevier, v.61, 4595 (2007).
22. M.Mai, C.Feldmann, *J. Mater. Sci.*, **47**, 1427 (2012).
23. V.S.Tinkova, A.G.Yakubovskaya, I.A.Tupitsyna et al., *Tekhnologiya i Konstruirovanie v Elektronnoi Apparature*, **1–2**, 40 (2019).
24. A.Tupitsyna, P.O.Maksimchuk, A.G.Yakubovskaya et al., *Functional Materials*, **24**, 16 (2017).
25. D.Spassky, S.Omelkov, H.Magi et al., *Opt. Mat.*, **36**, 1660 (2014).
26. A.Yakubovskaya, I.Tupitsyna, D.Sofronov et al., *Functional Materials*, **20**, 523 (2013).
27. Q.Dai, H.Song, X.Bai et al., *J. Phys, Chem, C*, **111**, 7586 (2007).
28. I.A.Tupitsyna, P.O.Maksimchuk, A.G.Yakubovskaya et al., *Functional Materials*, **23**, 535 (2016).